Rapid Communications | Editors' Suggestion

Three-dimensional superconducting gap in FeSe from angle-resolved photoemission spectroscopy

Y. S. Kushnirenko,[1] A. V. Fedorov,[1] E. Haubold,[1] S. Thirupathaiah,[1,2] T. Wolf,[3] S. Aswartham,[1] I. Morozov,[1,4] T. K. Kim,[5] B. Büchner,[1] and S. V. Borisenko[1]

[1]*IFW Dresden, Helmholtzstrasse 20, 01069 Dresden, Germany*

[2]*Solid State and Structural Chemistry Unit, Indian Institute of Science, Bangalore, Karnataka 560012, India*

[3]*Institute for Solid State Physics, Karlsruhe Institute of Technology, 76131 Karlsruhe, Germany*

[4]*Lomonosov Moscow State University, Moscow 119991, Russia*

[5]*Diamond Light Source, Harwell Campus, Didcot OX11 0DE, United Kingdom*

(Received 27 February 2018; revised manuscript received 19 April 2018; published 2 May 2018)

We present a systematic angle-resolved photoemission spectroscopy study of the superconducting gap in FeSe. The gap function is determined in a full Brillouin zone including all Fermi surfaces and k_z dependence. We find significant anisotropy of the superconducting gap in all momentum directions. While the in-plane anisotropy can be explained by both nematicity-induced pairing anisotropy and orbital-selective pairing, the k_z anisotropy requires an additional refinement of the theoretical approaches.

DOI: 10.1103/PhysRevB.97.180501

Detailed knowledge of the gap function in iron-based superconductors can help to identify the mechanism of superconductivity in these materials. Recent clarification of the details of the electronic structure in FeSe to a precision of 1 meV [1–12] is a necessary prerequisite to study the superconducting (SC) gap by angle-resolved photoemission spectroscopy (ARPES) and makes this material a perfect candidate for such a detailed investigation. There are several experimental studies of the superconducting gap in FeSe and closely related compounds using different techniques, including tunneling spectroscopy [13–19], ARPES [20–23], specific heat [24–26], and London penetration depth [16,26], but a consensus on the size and symmetry of the gap in the full Brillouin zone (BZ) has not yet been reached. Although ARPES still remains the only, though non-phase-sensitive, method of direct determination of the gap as a function of momentum, i.e., the gap function, the agreement between existing reports is far from perfect. For instance, the authors of Ref. [23] reported an isotropic 2.5 meV gap on a central pocket in $FeSe_{0.45}Te_{0.55}$, while smaller and considerably more anisotropic gaps in the compound with a very similar composition $FeSe_{0.4}Te_{0.6}$ are found in Ref. [22]. As for pristine FeSe, according to Ref. [21], the gap is anisotropic on a central holelike pocket, as well as in slightly S-doped FeSe [20], while no gap has been observed on the electron pockets in the corner of the BZ. This is in contrast to a majority of the tunneling results [13–16], which imply the presence of multiple superconducting gaps. Moreover, the specific heat and London penetration depth also indicate the presence of two gaps [26]. Finally, studies managing to shed light on a possible k_z dependence of the gap function are lacking, although it was mentioned in Ref. [20] that no gap could be detected either on the electronlike Fermi surfaces (FSs) or on part of the holelike pocket near the Γ point. Therefore, it is important to have precise information about the behavior of the gap function throughout the whole BZ, preferably obtained by the same technique.

In this Rapid Communication, we report the results of a high-resolution ARPES study of the superconducting gap function in single crystals of FeSe, exactly from the same material in which we recently clarified the fine details of the electronic structure [1,2,27]. We clearly observed two anisotropic SC gaps on hole- and electronlike Fermi surfaces. Their momentum variation as a function of k_x, k_y, and k_z is compared to the ones predicted by orbital-selective pairing [14] and nematicity-induced anisotropy of the pairing gap [28].

ARPES data have been collected at I05 beamline of Diamond Light Source [29]. Single-crystal samples were cleaved *in situ* in a vacuum of better than 2×10^{-10} mbar and measured at temperatures ranging from 5.7 K. Measurements were performed using linearly polarized synchrotron light, utilizing a Scienta R4000 hemispherical electron energy analyzer with an angular resolution of 0.2°–0.5° and an energy resolution of 3 meV. Samples were grown by the $KCl/AlCl_3$ chemical vapor transport method.

In Figs. 1(a)–1(f) we show the experimental Fermi surface maps of electron- and holelike pockets measured with different photon energies which correspond to different k_z values in a three-dimensional (3D) BZ. All maps were measured with linear horizontal polarized light. A schematic picture of the 3D Fermi surface of FeSe summarizing these and previous ARPES results is presented in Fig. 1(g) and evidence for the sensitivity of our experiments to the superconductivity itself is given in Figs. 1(h) and 1(i).

In the center of the BZ near the Z point, we see two holelike elliptical pockets crossing each other [Fig. 1(f)]. These two ellipses originate from two different domain orientations in the nematic state [1,3–5,8,20]. As one approaches the Γ point, the size of these holelike pockets squeezed by nematicity rapidly decreases, resulting in a very small FS at $k_z = 0$, as shown in Fig. 1(e). The intensity distribution along the cut through the FS centered at the Z point clearly shows two sets of spin-orbit split $d_{xz,yz}$ dispersing features in Fig. 1(h) while the d_{xy} band,

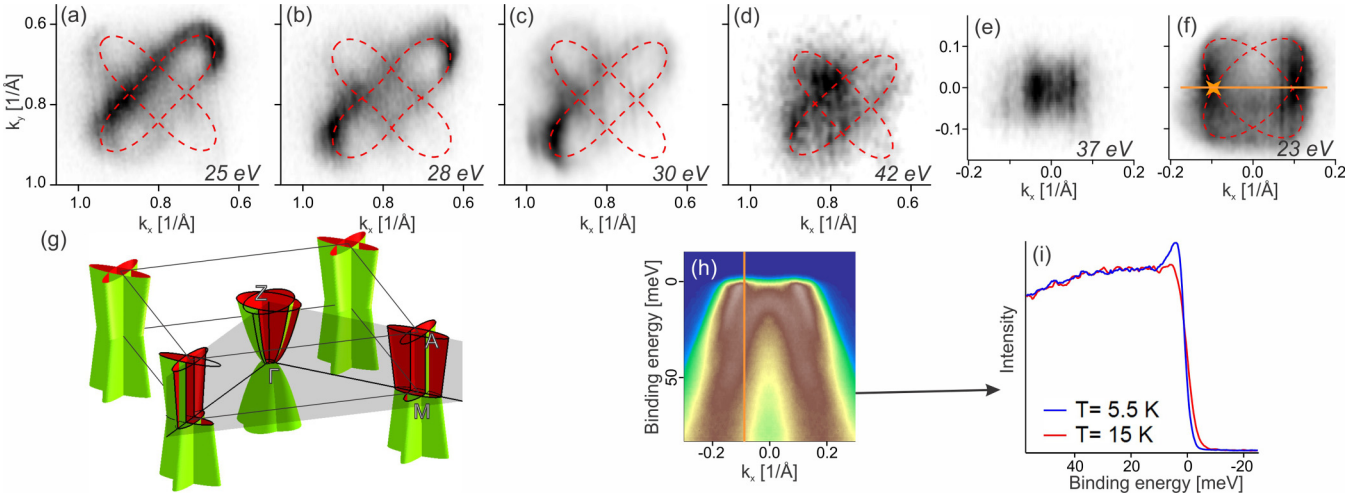

FIG. 1. (a)–(d) Fermi surface maps of the electronlike pockets measured using different photon energies. (e), (f) Fermi surface maps of the holelike pockets measured using different photon energies. (g) Schematic sketch of the experimentally determined 3D Fermi surface of FeSe. (h) Momentum-energy intensity distribution along the line indicated in (f), (i) k_F energy distribution curves above and below T_c corresponding to the line from (h) and a star from (f).

which tops in FeSe at 50 meV below the Fermi level, is hardly visible. The two features dispersing towards the Fermi level do not actually cross it and demonstrate all typical signs of the opening of a small superconducting gap. Direct evidence is given in Fig. 1(i) by two energy distribution curves (EDCs) taken above and below the critical temperature of FeSe. The emergence of a coherence peak as well as a typical shift of the leading-edge midpoint are clearly observed. Because of the closely separated multiple features with drastically different Fermi velocities close to the Fermi level, it is the shift of the leading edge, or leading-edge gap (LEG), which we will use throughout this Rapid Communication to characterize the superconducting gap in FeSe.

In the corner of the BZ, there are two peanutlike [30] pockets crossing each other [Figs. 1(a)–1(d) and 1(g)]. The size of these electronlike Fermi surfaces is also changing with k_z. A popular interpretation [5,7,8,11] of the presence of these two pockets is that they are the result of the superposition of single electron pockets from different domains of the twinned sample, as is the case with the hole pockets (see above). Our interpretation is that both pockets remain present also in the nematic phase, but they are slightly distorted. In this case the overlap of the signal from two domains leads to doubling of each peanut (see Supplemental Material [30]). In order to avoid additional complications with the extraction of gap values from the spectra, we adjust the photon energy and geometry of the experiment such that only one set of pockets is visible at a time.

Now let us turn to the momentum variation of the superconducting gap on the electronlike pocket near the A point. The data set shown in Fig. 2(a) was measured using 28 eV photons [30] with linear horizontal polarization from the sample cooled down to 5.5 K, i.e., in its superconducting state. We deliberately took the scans in a direction perpendicular to the BZ borders. Such experimental geometry allowed us to detect more spectral weight and thus more details. Specifically, the photoemission intensity from the pockets' ends is not suppressed as in the previous ARPES studies of the SC gap in FeSe and even some parts of the other pocket are visible. First, we establish the presence of a superconducting gap also in this region of momentum space. Figures 2(c) and 2(d) show k_F EDCs from places on the pocket marked with stars on Fig. 2(a) in the normal and the superconducting state. In both cases, the pairs of EDCs demonstrate the shift of the leading-edge position to higher binding energies upon entering the superconducting state. Moreover, this shift is not the same—it is equal to 0.3 and 0.6 meV, respectively—which indicates that the gap is not isotropic.

For a further analysis of gap anisotropy we have extracted the binding energy of the leading edge along the most intense

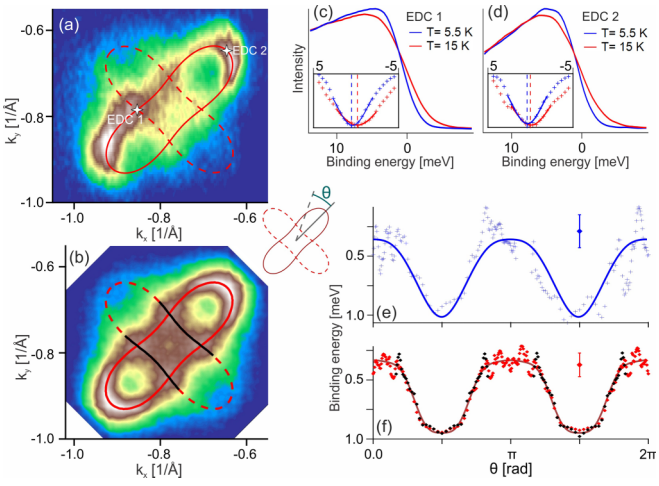

FIG. 2. (a) Fermi surface map of the electronlike pocket near the A point. (b) The map from (a), symmetrized about both axes of symmetry of the peanut. (c), (d) k_F energy distribution curves from parts of the pocket marked by stars in (a) measured in the normal and superconducting states. The insets show the first derivatives of the same curves. (e) Binding energy of the leading edge of k_F EDCs on the electronlike pocket from raw data. (f) The same as (e) but from the symmetrized data set. In order to match results from two different ellipses, the black dots are shifted by 90°.

peanut pocket. The result is shown in Fig. 2(e). Already, these results obtained from the raw data clearly demonstrate the presence of a noticeable gap anisotropy. To compensate for the matrix element effects, which result in an uneven intensity distribution along the peanut, we symmetrized the data set from Fig. 2(a). A symmetrized FS map is shown in Fig. 2(b) and the corresponding binding energy of the leading edge as a function of θ is shown in Fig. 2(f). Here, the red dots correspond to an ellipse from the map with a red contour on top, while the black dots correspond to a visible part of another peanut (black lines in the map). This plot presents direct evidence of an anisotropic superconducting gap on the electronlike pocket near the A point of FeSe. Not surprisingly, the symmetry of this gap function is C_2. The largest gap, which corresponds to the lowest leading-edge position, is on the shorter axis of the peanuts while the gap minima are on the longer axis of the peanuts. Fitting the data with a periodic function $\epsilon = A_0 + A_1\cos(2\phi) + A_2\cos(4\phi)$, where A_0, A_1, A_2 are free parameters, gives the amplitude of the gap variation of 0.6 meV [see the brown curve in Fig. 2(f)]. The fit to the raw data from the nonsymmetrized map has almost the same shape and amplitude [blue curve in Fig. 2(e)].

As mentioned above, each peanut of the electronlike FS is a superposition of two components which originate from two orthorhombic domains [30]. It is thus instructive to know exactly which component is analyzed in Fig. 2. From a comparison of the pocket shape obtained from Fig. 2(a) with the one in Ref. [30], one can conclude that intensity on this map mostly originates from the shorter peanut and we thus have analyzed the gap anisotropy related to this pocket. Because of the presence of the finite intensity from the longer peanut, the amplitude of the LEG gap anisotropy can be underestimated [30]. Here, we would like to point out that although LEG is a good qualitative measure of the superconducting gap and its anisotropy, the correspondence of the absolute values is more complicated and depends on many factors [31]. Since modeling of the spectral function, definitely necessary to provide (model-dependent) absolute values of the gap in the case of FeSe, is beyond the scope of this Rapid Communication, we will continue to discuss LEG as a robust quantity, which can be extracted directly from the raw data without a sophisticated data analysis. As a rule, the real gap is slightly larger than LEG.

To explore the gap function in whole 3D momentum space, we have also analyzed the data sets taken using different photon energies: 42 eV, which corresponds to the M point, 25 eV, and 30 eV. The amplitude of the LEG variation, i.e., the difference in the leading-edge position between the long and short peanut axis k_F EDCs, is given in Table I. While the functional form of the anisotropy is approximately the same, there are clear

TABLE I. Leading-edge gap anisotropy on the electronlike pocket for different k_z values.

Photon energy	Leading-edge gap anisotropy
25 eV	0.35 ± 0.1 meV
28 eV (A point)	0.6 ± 0.05 meV
30 eV	0.8 ± 0.1 meV
42 eV (M point)	0.7 ± 0.15 meV

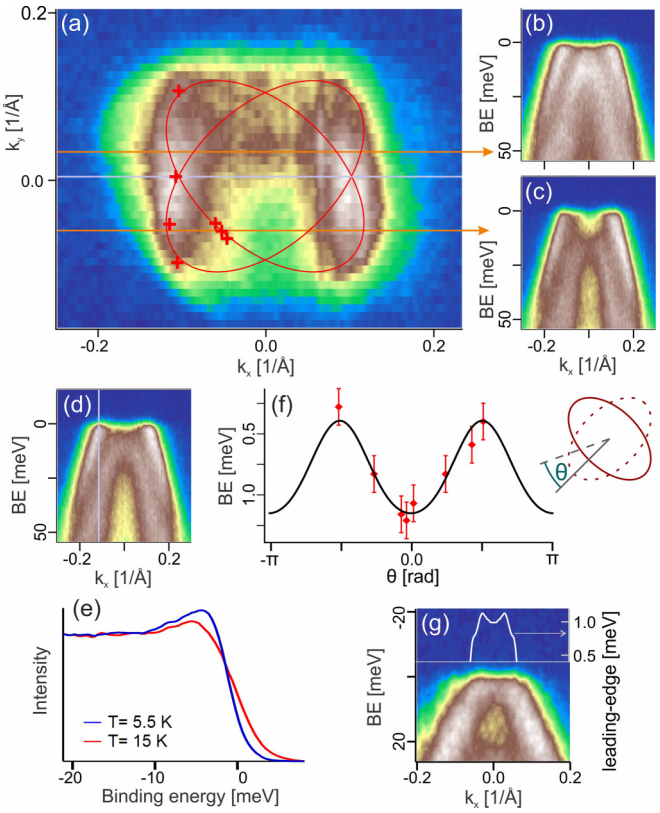

FIG. 3. (a) Fermi surface map of the holelike pocket near the Z point. (b)–(d) Spectra measured in directions shown on the map with two orange lines and one gray line, respectively. (e) k_F energy distribution curves obtained in a direction shown with a line on (d) from spectra measured in the normal and superconducting state. (f) Binding energy of the leading edge of the k_F EDCs from the holelike pocket. (g) Cut through the Γ point with the white line representing the leading-edge position of EDCs near zero momentum.

oscillations of the amplitude as a function of k_z with the most rapid variations taking place in the vicinity of the A point.

Now let us consider the holelike Fermi surface in the center of the Brillouin zone. Figure 3(a) shows a Fermi surface map of the holelike pocket near the Z point. Here, it is convenient to analyze the EDCs from the lower part of the map, as Figs. 3(b) and 3(c) demonstrate. In Fig. 3(b) the cut from the upper part of the map is shown where it is seen that the other split component of $d_{xz,yz}$ dispersion is strong and thus complicates the LEG analysis. In Fig. 3(c), in contrast, the intensity from these states is weak and the dispersing features responsible for the gapped FS are more pronounced. The presence of the gap is evident from Fig. 3(e), which shows k_F EDCs from an intensity distribution along the line going through the Z point [Fig. 3(d)] measured above and below T_c. The leading-edge shift between these EDCs is 0.8 meV. In order to estimate the SC gap anisotropy on this FS, we have extracted the binding energy of the leading edge from the exemplary EDCs corresponding to the red markers in Fig. 3(a). The result is shown in Fig. 3(f). Also from this figure one clearly notices that the gap on the holelike pocket is anisotropic, with a maximum located on the shorter ellipse axis and minimum on the longer one. Fitting

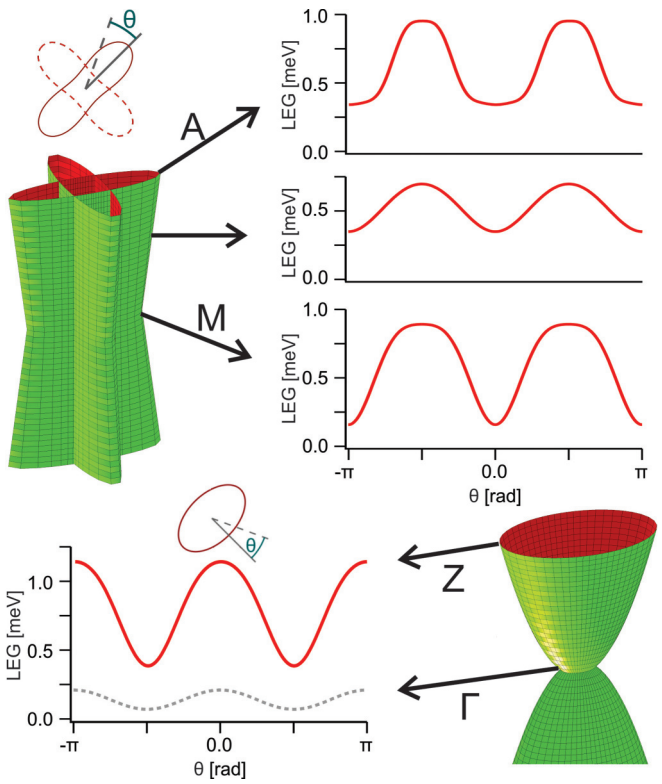

FIG. 4. Summary of the obtained results. The fits to the experimental LEG distribution in 3D BZ are shown for different k_z values for hole and electron pockets. In both cases, zero θ corresponds to the diagonal of the BZ, i.e., the direction in the momentum space which connects the center of the holelike pocket with the center of the electronlike pocket. The curve corresponding to the gap behavior around the G-point is dashed to emphasize the higher experimental uncertainty.

the data with a periodic function yields a difference between extrema of 0.75 ± 0.1 meV.

Near the Γ point the holelike pocket becomes too small (about 0.06 Å^{-1} in diameter) to disentangle two components of the Fermi surface originating from two domain orientations. Analysis of the asymmetry of the superconducting gap becomes very complicated and model dependent. The presence of the gap itself is apparent, though. This follows also from the typical leading-edge position behavior extracted from the cut measured through the pocket center [Fig. 3(g)]. The presence of a deep minimum in this curve points to the backfolding of the dispersion due to superconductivity. If the top of the dispersion is located close to the Fermi level, as is the case here, opening of the gap results exactly in this behavior of the leading-edge position [32]. In the case of the absence of the gap, i.e., nodes, one would expect the flat shape of this curve to be dictated mostly by the Fermi function since the spectral function is nearly equally strong also in between the Fermi level crossings due to its proximity to the top.

Figure 4 summarizes our findings as regards the 3D gap function in FeSe. In this figure we show only the FS corresponding to a single domain. The superconducting gap on both parts of the Fermi surface is anisotropic in the k_x-k_y plane as well as in the k_z direction. The largest leading-edge gap is on the holelike pocket near the Z point. The gap oscillations on this pocket have C_2 symmetry with a maximum on a short axis of the ellipse. Near the Γ point the gap seems to be considerably smaller but not zero. Since we did not manage to observe clear coherence peak in the regions of maximal gap, the degree of anisotropy may be higher. A symmetry of the leading-edge gap on the electronlike pocket also has C_2 behavior on each of the two ellipses. Its highest value corresponds to the short axis of the ellipse and is smaller than the one on the holelike pocket. The behavior of the gap on the electronlike pocket is qualitatively the same for all k_z, but is characterized by a nonmonotonic amplitude of the oscillations when going from the A to the M point.

We have previously detected a correlation between the size of the gap and degree of spin-orbit splitting in all main representatives of iron-based superconductors [2]. The present study confirms this with a different level of precision for FeSe. Indeed, the absolute value of the gap in the center of the BZ, where spin-orbit splitting is maximal, is larger than the one on the electronlike pockets. Another correlation with the absolute value of the gap has been noticed by us in hole-doped 122 materials [33]. There, we have demonstrated that the gap is always the largest for the $d_{xz,yz}$ states and decreases as soon as the other orbital character is admixed.

We also compare the earlier determined anisotropic gap function in LiFeAs [34] with the one determined in the present study in FeSe. Apparently, very different electronic structures result in qualitatively different gap structures. In the case of LiFeAs, electronlike pockets are significantly larger and the gap oscillates on them in phase, having C_4 symmetry, i.e., it is maximal on both of them when crossing the diagonal of the BZ and is minimal in between, regardless of the shorter or longer axes of the ellipses. The gap of $d_{xz,yz}$ states is also the largest in FeSe but oscillates in the same way as the gap on the large d_{xy} pocket in LiFeAs (which is absent in FeSe) having minima on the diagonals of the BZ. Oscillations of the gap on small and 3D $d_{xz,yz}$ pockets in LiFeAs have not been resolved. This comparison calls for detailed and quantitative theoretical estimates of the gaps in FeSe by the same methods applied earlier to LiFeAs [35–37].

The presented results imply a significant anisotropy of the superconducting gap in FeSe, not only in plane, but also as a function of k_z. This is in contrast to the expectations of the conventional spin-fluctuation-mediated pairing theories where mostly isotropic s-wave gaps are expected, or anisotropy is different. The concept of orbital-selective Cooper pairing suggested recently [14,38] seems to be in agreement with our observations: The anisotropy of the superconducting gap in FeSe studied by us can be roughly explained by the orbital composition of the states forming the Fermi surface in the normal state. As soon as the contribution of the $d_{xz,yz}$ character is stronger, the gap reaches its maximum. On the other hand, this concept also requires adding phenomenologically different quasiparticle spectral weights for the d_{xz} and d_{yz} orbitals. We do not observe significantly different Z weights of these orbitals, because both electronlike pockets are present within a single domain and the corresponding peaks of the spectral function are equally sharp [30]. At the same time, our results are in a qualitative agreement with the gap anisotropy extracted from the tunneling data [14], with the difference in the absolute values being probably due to the mentioned peculiarities of the LEG.

Our data are also in agreement with the variations of the pairing gap caused by nematicity itself [28]. In this approach, the anisotropy of the gap arises from the mixing of s-wave and d-wave pairing channels without the need to postulate different Z factors for each orbital.

In order to make a more rigorous statement regarding the application of one or another theoretical approach, more detailed calculations are obviously needed to reproduce the whole 3D momentum dependence of the superconducting gap in FeSe determined in the present study.

This work was supported by DFG No. BO1912/6-1. We acknowledge Diamond Light Source for time on Beamline I05 under Proposals No. SI11643-1 and No. SI18586-1. We are grateful to D. Morr, M. Watson, A. Chubukov, and A. Kordyuk for fruitful discussions.

[1] A. Fedorov, A. Yaresko, T. K. Kim, Y. Kushnirenko, E. Haubold, T. Wolf, M. Hoesch, A. Grueneis, B. Büchner, and S. Borisenko, Sci. Rep. **6**, 36834 (2016).

[2] S. V. Borisenko, D. V. Evtushinsky, Z.-H. Liu, I. Morozov, R. Kappenberger, S. Wurmehl, B. Büchner, A. N. Yaresko, T. K. Kim, M. Hoesch *et al.*, Nat. Phys. **12**, 311 (2016).

[3] M. D. Watson, T. K. Kim, L. C. Rhodes, M. Eschrig, M. Hoesch, A. A. Haghighirad, and A. I. Coldea, Phys. Rev. B **94**, 201107(R) (2016).

[4] Y. V. Pustovit and A. A. Kordyuk, Low Temp. Phys. **42**, 995 (2016).

[5] M. D. Watson, T. K. Kim, A. A. Haghighirad, N. Davies, A. McCollam, A. Narayanan, S. F. Blake, Y. L. Chen, S. Ghannadzadeh, A. J. Schofield *et al.*, Phys. Rev. B **91**, 155106 (2015).

[6] M. D. Watson, T. K. Kim, A. A. Haghighirad, S. F. Blake, N. R. Davies, M. Hoesch, T. Wolf, and A. I. Coldea, Phys. Rev. B **92**, 121108(R) (2015).

[7] P. Zhang, T. Qian, P. Richard, X. Wang, H. Miao, B. Lv, B. Fu, T. Wolf, C. Meingast, X. Wu *et al.*, Phys. Rev. B **91**, 214503 (2015).

[8] Y. Suzuki, T. Shimojima, T. Sonobe, A. Nakamura, M. Sakano, H. Tsuji, J. Omachi, K. Yoshioka, M. Kuwata-Gonokami, T. Watashige *et al.*, Phys. Rev. B **92**, 205117 (2015).

[9] Z. R. Ye, C. F. Zhang, H. Ning, W. Li, L. Chen, T. Jia, M. Hashimoto, D. H. Lu, Z.-X. Shen, and Y. Zhang, arXiv:1512.02526.

[10] K. Nakayama, Y. Miyata, G. N. Phan, T. Sato, Y. Tanabe, T. Urata, K. Tanigaki, and T. Takahashi, Phys. Rev. Lett. **113**, 237001 (2014).

[11] T. Shimojima, Y. Suzuki, T. Sonobe, A. Nakamura, M. Sakano, J. Omachi, K. Yoshioka, M. Kuwata-Gonokami, K. Ono, H. Kumigashira *et al.*, Phys. Rev. B **90**, 121111(R) (2014).

[12] J. Maletz, V. Zabolotnyy, D. Evtushinsky, S. Thirupathaiah, A. Wolter, L. Harnagea, A. Yaresko, A. Vasiliev, D. Chareev, A. Böhmer *et al.*, Phys. Rev. B **89**, 220506(R) (2014).

[13] L. Jiao, C.-L. Huang, S. Rößler, C. Koz, U. K. Rößler, U. Schwarz, and S. Wirth, Sci. Rep. **7**, 44024 (2017).

[14] P. O. Sprau, A. Kostin, A. Kreisel, A. E. Böhmer, V. Taufour, P. C. Canfield, S. Mukherjee, P. J. Hirschfeld, B. M. Andersen, and J. S. Davis, Science **357**, 75 (2017).

[15] S. A. Moore, J. L. Curtis, C. Di Giorgio, E. Lechner, M. Abdel-Hafiez, O. S. Volkova, A. N. Vasiliev, D. A. Chareev, G. Karapetrov, and M. Iavarone, Phys. Rev. B **92**, 235113 (2015).

[16] S. Kasahara, T. Watashige, T. Hanaguri, Y. Kohsaka, T. Yamashita, Y. Shimoyama, Y. Mizukami, R. Endo, H. Ikeda, K. Aoyama *et al.*, Proc. Natl. Acad. Sci. U.S.A. **111**, 16309 (2014).

[17] U. R. Singh, S. C. White, S. Schmaus, V. Tsurkan, A. Loidl, J. Deisenhofer, and P. Wahl, Phys. Rev. B **88**, 155124 (2013).

[18] C.-L. Song, Y.-L. Wang, P. Cheng, Y.-P. Jiang, W. Li, T. Zhang, Z. Li, K. He, L. Wang, J.-F. Jia *et al.*, Science **332**, 1410 (2011).

[19] T. Watashige, Y. Tsutsumi, T. Hanaguri, Y. Kohsaka, S. Kasahara, A. Furusaki, M. Sigrist, C. Meingast, T. Wolf, H. v. Löhneysen *et al.*, Phys. Rev. X **5**, 031022 (2015).

[20] H. Xu, X. Niu, D. Xu, J. Jiang, Q. Yao, Q. Chen, Q. Song, M. Abdel-Hafiez, D. Chareev, A. Vasiliev *et al.*, Phys. Rev. Lett. **117**, 157003 (2016).

[21] T. Hashimoto, Y. Ota, H. Q. Yamamoto, Y. Suzuki, T. Shimojima, S. Watanabe, C. Chen, S. Kasahara, Y. Matsuda, T. Shibauchi *et al.*, Nat. Commun. **9**, 282 (2018).

[22] K. Okazaki, Y. Ito, Y. Ota, Y. Kotani, T. Shimojima, T. Kiss, S. Watanabe, C.-T. Chen, S. Niitaka, T. Hanaguri *et al.*, Phys. Rev. Lett. **109**, 237011 (2012).

[23] H. Miao, P. Richard, Y. Tanaka, K. Nakayama, T. Qian, K. Umezawa, T. Sato, Y.-M. Xu, Y. Shi, N. Xu *et al.*, Phys. Rev. B **85**, 094506 (2012).

[24] Y. Sun, A. Park, S. Pyon, T. Tamegai, and H. Kitamura, Phys. Rev. B **96**, 140505 (2017).

[25] B. Zeng, G. Mu, H. Luo, T. Xiang, I. Mazin, H. Yang, L. Shan, C. Ren, P. Dai, and H.-H. Wen, Nat. Commun. **1**, 112 (2010).

[26] M. Abdel-Hafiez, Y.-Y. Zhang, Z.-Y. Cao, C.-G. Duan, G. Karapetrov, V. Pudalov, V. Vlasenko, A. Sadakov, D. Knyazev, T. Romanova *et al.*, Phys. Rev. B **91**, 165109 (2015).

[27] Y. S. Kushnirenko, A. A. Kordyuk, A. V. Fedorov, E. Haubold, T. Wolf, B. Büchner, and S. V. Borisenko, Phys. Rev. B **96**, 100504(R) (2017).

[28] J. Kang, R. M. Fernandes, and A. V. Chubukov, arXiv:1802.01048.

[29] M. Hoesch, T. K. Kim, P. Dudin, H. Wang, S. Scott, P. Harris, S. Patel, M. Matthews, D. Hawkins, S. G. Alcock *et al.*, Rev. Sci. Instrum. **88**, 013106 (2017).

[30] See Supplemental Material at http://link.aps.org/supplemental/10.1103/PhysRevB.97.180501 for we present additional data which imply that both electron pockets are present in a single-domain sample. There are also two remarks as for the extraction of the leading edge position and choice of photon energy.

[31] A. A. Kordyuk, S. V. Borisenko, M. Knupfer, and J. Fink, Phys. Rev. B **67**, 064504 (2003).

[32] D. V. Evtushinsky, T. K. Kim, A. A. Kordyuk, V. B. Zabolotnyy, B. Büchner, A. Boris, D. Sun, C. Lin, H. Luo, Z. Wang *et al.*, arXiv:1106.4584.

[33] D. V. Evtushinsky, V. B. Zabolotnyy, T. K. Kim, A. A. Kordyuk, A. N. Yaresko, J. Maletz, S. Aswartham, S. Wurmehl, A. V. Boris, D. L. Sun *et al.*, Phys. Rev. B **89**, 064514 (2014).

[34] S. V. Borisenko, V. B. Zabolotnyy, A. A. Kordyuk, D. V. Evtushinsky, T. K. Kim, I. V. Morozov, R. Follath, and B. Büchner, Symmetry **4**, 251 (2012).

[35] Y. Wang, A. Kreisel, V. B. Zabolotnyy, S. V. Borisenko, B. Buchner, T. A. Maier, P. J. Hirschfeld, and D. J. Scalapino, Phys. Rev. B **88**, 174516 (2013).

[36] T. Saito, S. Onari, Y. Yamakawa, H. Kontani, S. V. Borisenko, and V. B. Zabolotnyy, Phys. Rev. B **90**, 035104 (2014).

[37] F. Ahn, I. Eremin, J. Knolle, V. B. Zabolotnyy, S. V. Borisenko, B. Buchner, and A. V. Chubukov, Phys. Rev. B **89**, 144513 (2014).

[38] A. Kreisel, B. M. Andersen, P. O. Sprau, A. Kostin, J. C. S. Davis, and P. J. Hirschfeld, Phys. Rev. B **95**, 174504 (2017).